Sensors and Materials, Vol. 36, No. 1 (2024) 261–267
MYU Tokyo

S & M 3516

Recombination Dynamics of Electron–Hole Pairs in TlBr Crystals Probed by Transient Absorption Spectroscopy Using Pulsed Electron Beams

Masanori Koshimizu,[1*] Yusa Muroya,[2] Mitsuhiro Nogami,[3] and Keitaro Hitomi[3]

[1]Research Institute of Electronics, Shizuoka University, 3-5-1 Johoku, Naka-ku, Hamamatsu 432-8011, Japan
[2]Institute of Scientific and Industrial Research, Osaka University, 8-1 Mihogaoka, Ibaraki, Osaka 567-0047, Japan
[3]Department of Quantum Science and Energy Engineering, Graduate School of Engineering, Tohoku University, 6-6-01-2 Aoba, Aramaki, Aoba-ku, Sendai 980-8579, Japan

(Received October 5, 2023; accepted January 5, 2024)

Keywords: transient absorption, pulse radiolysis, TlBr, carrier recombination, semiconductor detector

To develop semiconductor detectors based on TlBr with excellent energy resolution at high yields, a variety of characterization methods for TlBr crystals are necessary. Among the various methods based on excitation by photons or ionizing radiation, we chose transient absorption measurements after the irradiation of pulsed electron beams to analyze the recombination dynamics of electron–hole pairs generated by the electron beams. The decay behavior of the transient absorption depended on the pulse intensity and was satisfactorily fitted with a decay function based on bimolecular recombination dynamics. The bimolecular recombination coefficients obtained from the fitting were similar for the samples cut from different parts of a crystal boule. Assuming that the recombination occurred through Shockley–Read–Hall bimolecular recombination via electronic levels of defects within the bandgap, the result indicates that the concentrations of the defects responsible for the recombination were similar for the samples out from different parts of the crystal boule.

1. Introduction

TlBr is an indirect-gap semiconductor with a bandgap energy of 2.7 eV. It has been attracting considerable attention for its application to radiation detectors owing to the room-temperature operation due to the large bandgap energy and high stopping power for high-energy photons such as X-rays and gamma rays.(1) High crystallinity and purity are necessary to achieve detectors with excellent energy resolution. At present, the yield of detector parts having excellent energy resolution from a grown crystal boule is limited, which is related to defects or impurities that prevent the collection of electron–hole pairs as the detection signal. Accordingly, various techniques have been employed to characterize the crystalline structure, including electron backscattered diffraction and positron annihilation.(2) Also, the dynamics and transport properties of electron–hole pairs in TlBr crystals have been characterized using

*Corresponding author: e-mail: koshimizu.masanori@shizuoka.ac.jp
https://doi.org/10.18494/SAM4694

ISSN 0914-4935
https://myukk.org/

photoconductivity,[3–8] photoluminescence,[9–11] cathodoluminescence,[12] and X-ray-induced radioluminescence.[10,13] We have recently applied pump-probe-type transient absorption spectroscopy to elucidate the dynamics of the electron–hole pairs produced by pulsed electron beams[14] we discussed the origin of the transient absorption and some of the dynamics. Herein, we focus on the intensity dependence of the dynamics to elucidate the recombination dynamics of electron–hole pairs.

2. Materials and Methods

The TlBr crystals used as samples were grown by the horizontal traveling molten zone method. The raw material (99.999%, Aldrich) was purified by 542-times zone melting with a furnace movement speed of 5 cm/h. After the zone melting, a crystal boule was grown by performing a single zone pass with a furnace movement speed at 1 mm/h. Crystals cut from different parts of this boule were used for the measurements. These samples are hereafter referred to as the start, middle, and end parts, which are located at 9.6–10.8, 44.0–45.2, and 78.4–79.6 mm from the start point of the growth, respectively. Both sides of the samples were polished. Details of the growth technique were reported previously.[1] The results for the three samples were similar; therefore, the results for the middle part are described unless otherwise mentioned.

Transient absorption spectroscopy was performed at the electron linear accelerator facility of the Institute of Scientific and Industrial Research, Osaka University, Japan. For the measurements at the nanosecond scale, electron beams with a pulse duration of 8 ns [full width at half maximum (FWHM)] were used. The probe light was generated using a Xe flash lamp (SA-200F, Nissin Electronic Co., Ltd.). The transmitted light at different wavelengths was obtained using monochromators (MC-10N, Ritu Oyo Kougaku Co., Ltd.). The transmitted light in the UV–VIS region (260–900 nm) and NIR region (900–1500 nm) was detected by a Si photodiode (S1722-02, Hamamatsu Photonics Co., Ltd.) and an InGaAs detector (DET-10C, Thorlabs Inc.), respectively. The detection signals, namely, time profiles of the transmitted light intensity, were recorded using a digital oscilloscope (DPO7254, Tektronix Inc.). On the basis of the difference in the time profile of the transmitted light with and without pulsed electron beam irradiation, the transient absorption time profiles were obtained at different wavelengths. Details can be found in a previous paper.[15] For the measurements at the picosecond scale, electron beams with a pulse duration of ~5 ps (FWHM) were used. The fundamental light of a Ti–sapphire laser (Tsunami, Spectra Physics Inc.) with a regenerative amplifier (Spitfire, Spectra Physics Inc.) was focused to a CaF_2 or sapphire crystal to obtain a pulsed white light as the probe light. The arrival timing of the probe light relative to the pulsed electron beam was changed using an optical delay line. The spectra of the transmitted probe light pulse were recorded using a multichannel CMOS detector (AvaSpec-ULS2048CL-EVO, Avantes). The transient absorption spectra were obtained from the transmitted light spectra with and without pulsed electron beam irradiation. The principle and setup of the picosecond pulse radiolysis experiment were previously reported.[16] The pulse intensity was changed by changing the bias voltage applied to the electron gun of the accelerator, and the pulse dose was estimated using the solvated electron yield in water.

3. Results and Discussion

The time-resolved transient absorption spectra of the TlBr crystal are shown in Fig. 1. A sharp peak was observed at 1160 nm, which is attributed to shallow trap sites.[12,14] In addition to the sharp peak, structureless absorption was observed at 400–800 nm and tentatively attributed to free carrier absorption. The spectra are consistent with those in a previous paper.[14] To avoid the contribution of shallow traps, we analyzed the free carrier dynamics at 600 nm.

The time profiles of the transient absorption at 600 nm at different pulse intensities in the nanosecond range are presented in Fig. 2. The decay rate of the transient absorption increased with the pulse intensity, which strongly suggests that the recombination rate of electron–hole pairs differed at different pulse intensities. This is not the case for first-order decay, in which the interaction between multiple electron–hole pairs is negligible. Assuming that the recombination

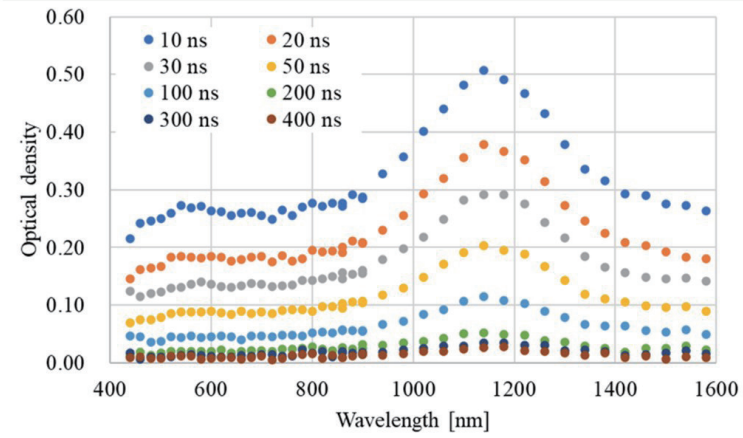

Fig. 1. (Color online) Time-resolved transient absorption spectra of TlBr crystal in the nanosecond range.

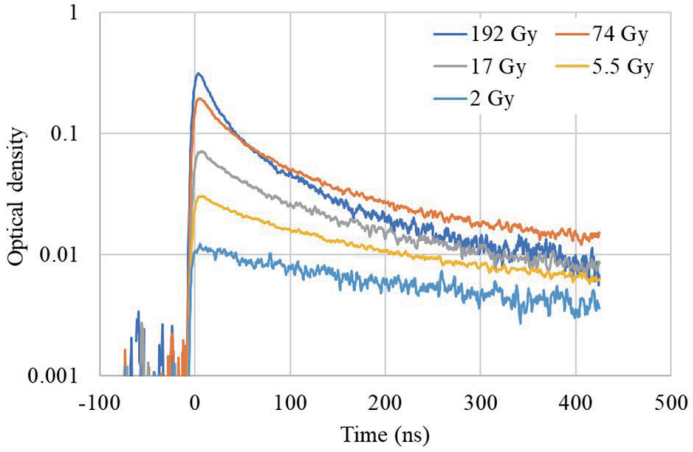

Fig. 2. (Color online) Transient absorption time profiles of TlBr crystal at different pulse intensities in the nanosecond range.

of electron–hole pairs is the cause of the decay, we consider the time dependence of the concentration of electron–hole pairs in a framework of bimolecular recombination of electron–hole pairs:

$$\frac{dC(t)}{dt} = -kC^2(t), \tag{1}$$

where $C(t)$ is the concentration of electron–hole pairs at time t after excitation by the pulsed electron beam and k represents the bimolecular recombination rate coefficient. Here, only excess densities of electrons and holes are considered. Equation (1) can be rewritten as

$$\frac{dC(t)}{C^2(t)} = -kdt. \tag{2}$$

The integration of both sides of Eq. (2) from $t = 0$ to $t = t$ gives

$$\frac{1}{C(0)} - \frac{1}{C(t)} = -kt, \tag{3}$$

which can be rewritten as

$$C(t) = \frac{1}{kt + 1/C(0)}. \tag{4}$$

If we assume that the transient absorption is proportional to the concentration of electron–hole pairs, the decay behaviors of the transient absorption can be fitted with Eq. (4).

The time profiles of the transient absorption at 600 nm at different pulse intensities in the nanosecond range and the function fitted using Eq. (4) are presented in Fig. 3. The decay behaviors at different pulse intensities are satisfactorily fitted with the equation, which indicates that the decay behaviors are well represented by the bimolecular recombination of electron–hole pairs. Similar results were obtained for the start and end parts of the crystal boule.

Using the fitting procedure, we estimated the bimolecular recombination coefficient k and the initial concentration $C(0)$ of electron–hole pairs in an arbitrary unit. Unfortunately, the concentration of electron–hole pairs could not be correctly estimated because the absorbance of electron–hole pairs at a given concentration was unknown. The estimated bimolecular recombination coefficients of the different parts of the crystal are shown in Fig. 4. The bimolecular recombination coefficient changed with the pulse intensity for all samples, possibly owing to the low signal-to-noise ratio at a low pulse intensity. At the highest pulse intensity, the bimolecular recombination coefficient was $2.2 \pm 0.2 \times 10^8$ cm^{-3} s^{-1}. Assuming that the carrier density decreased through Shockley–Read–Hall bimolecular recombination,[3] in which

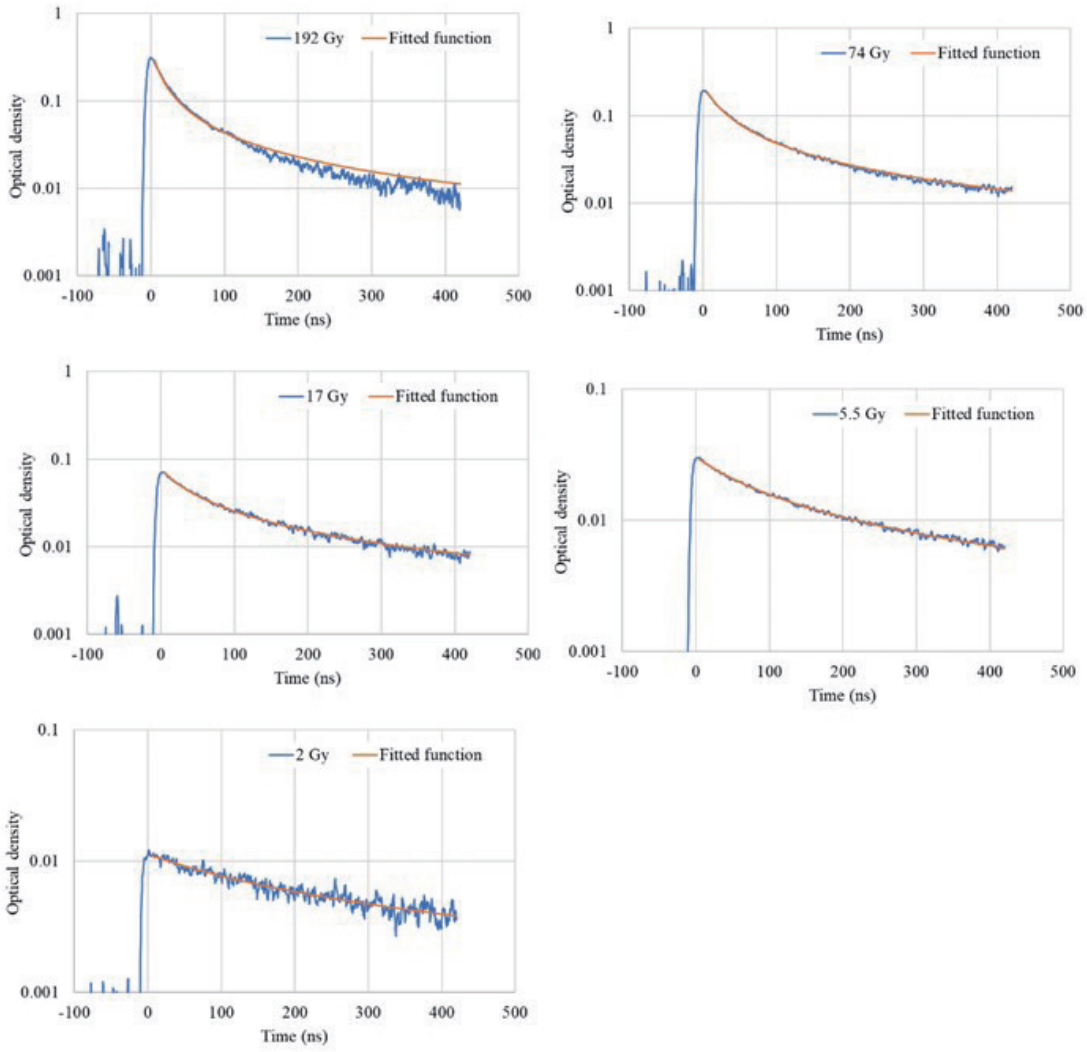

Fig. 3. (Color online) Transient absorption time profiles of TlBr crystal at different pulse intensities in the nanosecond range and fitted function using Eq. (4).

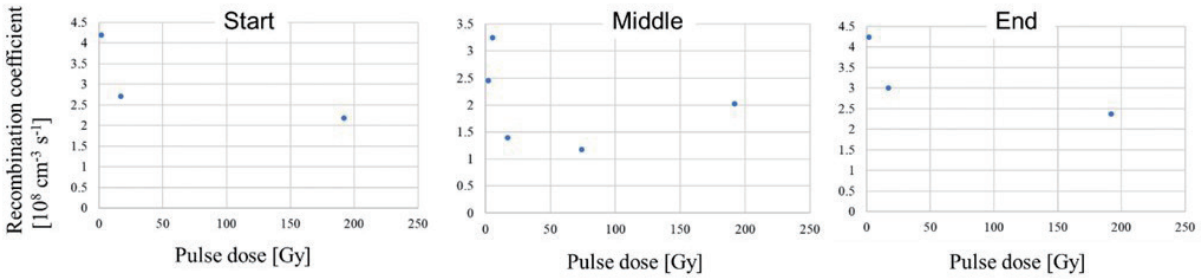

Fig. 4. (Color online) Bimolecular recombination coefficients at different pulse intensities in different parts of the crystal boule.

recombination occurs via electronic levels of defects within the bandgap, similar recombination coefficients indicate that the concentrations of the defects involved in the recombination were similar in the different samples. There is a possibility of the contribution of Auger recombination in the analysis. Indeed, the fitted result has a slight discrepancy at the tail of the decay at the highest dose of 192 Gy as shown in Fig. 3. If the Auger recombination also contributes to the recombination, the additional recombination channel due to the Auger recombination accelerates the decay, which may result in an overestimation of the recombination coefficient. The initial concentration of electron–hole pairs in the arbitrary unit for the different samples as a function of pulse intensity is presented in Fig. 5. Note that the initial concentration of electron–hole pairs did not increase linearly with the pulse intensity. One possible reason for this deviation from linearity at a high pulse intensity is Auger recombination, whose contribution in the rate equation is proportional to the third power of the concentration of electron–hole pairs.[17]

The time profiles of the transient absorption at 600 nm at different pulse intensities in the picosecond range are presented in Fig. 6. For the pulse intensity of 49 Gy, the optical density significantly decreased up to 8 ns, whereas a negligible decrease was observed for the pulse intensity of 20 Gy. This difference in initial decay may also be the cause of the sublinear dependence of the initial concentration of electron–hole pairs shown in Fig. 5.

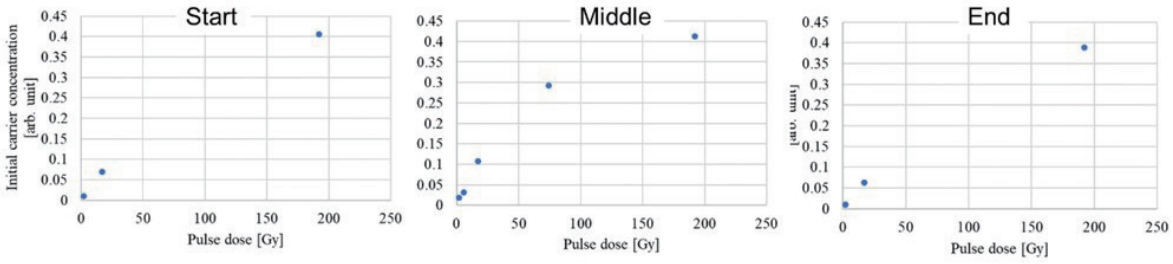

Fig. 5. (Color online) Initial concentration of electron–hole pairs in arbitrary unit as function of pulse intensity for different samples.

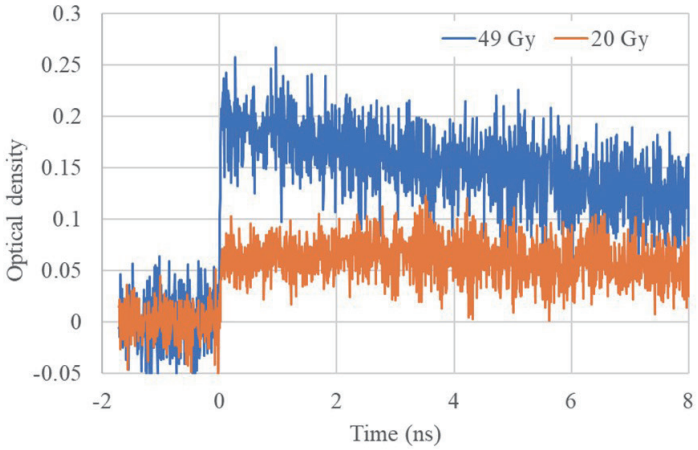

Fig. 6. (Color online) Transient absorption time profiles of TlBr crystal at different pulse intensities in the picosecond range.

4. Conclusions

We analyzed the transient absorption characteristics of TlBr crystals after the irradiation of pulsed electron beams. The decay behaviors in the nanosecond range were described in terms of bimolecular recombination dynamics. By fitting the decay behaviors, we elucidated the bimolecular recombination coefficients and initial concentration of electron–hole pairs in an arbitrary unit. Assuming that the decay is due to Shockley–Read–Hall bimolecular recombination, in which recombination occurs via electronic levels of defects within the bandgap, similar bimolecular recombination coefficients for different samples indicate that the concentrations of the defects responsible for the recombination were similar in the samples. The results presented in this paper indicate that the contribution of the defect-mediated recombination of electron–hole pairs can be monitored using the transient absorption.

Acknowledgments

This research was supported by a Grant-in-Aid for Scientific Research (A) (No. 19H00880, 2019–2022) and the Takayanagi Memorial Fund for the Creation of Future Technology. Part of this research is based on the Cooperative Research Project of Research Center for Biomedical Engineering, Ministry of Education, Culture, Sports, Science and Technology of Japan. This work was performed under the Cooperative Research Program "Network Joint Research Center for Materials and Devices."

References

1 K. Hitomi, T. Shoji, and K. Ishii: J. Cryst. Growth **379** (2013) 93.
2 M. Zhang, Z. Zheng, Z. Chen, S. Zhang, W. Luo, Q. Fu, J. Cryst. Growth **487** (2018) 8.
3 D. R. Onken, S. Gridin, K. B. Ucer, R. T. Williams, A. Datta, and S. Motakef, Proc. SPIE 10392, Hard X-Ray, Gamma-Ray, and Neutron Detector Physics XIX, 1039212 (29 August 2017). https://doi.org/10.1117/12.2276866
4 V. Kazukauskas, A. Ziminskij, G. Davidyuk, V. Bozhko, and G. Mironchuk: Phys. Status Solidi C **6** (2009) 2795.
5 J. Vaitkus, V. Gostilo, R. Jasinskaite, A. Mekys, A. Owens, S. Zatoloka, and A. Zindulis: Nucl. Instrum. Methods Phys. Res. A **531** (2004) 192.
6 J. Vaitkus, J. Banys, V. Gostilo, S. Zatoloka, A. Mekys, J. Storasta, and A. Zinduli: Nucl. Instrum. Methods Phys. Res. A **546** (2005) 188.
7 V. Kazukauskas, A. Ziminskij, G. Davidyuk, V. Bozhko, and G. Mironchuk: Mol. Cryst. Liq. Cryst. **522** (2010) 82.
8 V. Kažukauskas, R. Garbačauskas, S. Savicki, V. Gostilo, and M. Shorohov: Mol. Cryst. Liq. Cryst. **655** (2017) 142.
9 K. Hayakawa, K. Hitomi, T. Shoji, and C Onodera: IEEE Trans. Nucl. Sci. Sym. Conf. (2009) Record N25-172.
10 M. Koshimizu, K. Hitomi, M. Nogami, T. Yanagida, Y. Fujimoto, and K. Asai: Jpn. J. Appl. Phys. **59** (2020) SCCB19.
11 L. Grigorjeva and D. Millers: Nucl. Instrum. Methods Phys. Res., Sect. B **191** (2002) 131.
12 L. Grigorjeva, D. Millers, M. Shorohov, I. S. Lisitskii, M. S. Kuznetsov, S. Zatoloka, and V. Gostilo: Nucl. Instrum. Methods Phys. Res., Sect. A **531** (2004) 197.
13 M. Shorohov, L. Grigorjeva, and D. Millers: Nucl. Instrum. Methods Phys. Res., Sect. A **563** (2006) 78.
14 M. Koshimizu, Y. Muroya, S. Yamashita, M. Nogami, K. Hitomi, Y. Fujimoto, and K. Asai: Sens. Mater. **32** (2020) 1445.
15 K. Kobayashi and S. Tagawa: J. Am. Chem. Soc. **125** (2003) 10213.
16 A. Saeki, T. Kozawa, K. Okamoto, and S. Tagawa: Jpn. J. Appl. Phys. **46** (2007) 407.
17 J. Q. Grim, K. B. Ucer, A. Burger, P. Bhattacharya, E. Tupitsyn, E. Rowe, V. M. Buliga, L. Trefilova, A. Gektin, G. A. Bizarri, W. W. Moses, and R. T. Williams, Phys. Rev. B **87** (2013) 125117.